Published in final edited form as:
Sci Transl Med. 2012 June 20; 4(139): 139ra85. doi:10.1126/scitranslmed.3003921.

Recombinant MG53 protein modulates therapeutic cell membrane repair in treatment of muscular dystrophy

Noah Weisleder[1,2,*], **Norio Takizawa**[2], **Peihui Lin**[1], **Xianhua Wang**[3], **Chunmei Cao**[3], **Yan Zhang**[3], **Tao Tan**[2], **Christopher Ferrante**[2], **Hua Zhu**[1], **Pin-Jung Chen**[2], **Rosalie Yan**[2], **Matthew Sterling**[1], **Xiaoli Zhao**[1], **Moonsun Hwang**[1], **Chuanxi Cai**[1], **Heping Cheng**[3], **Hiroshi Takeshima**[4], **Ruiping Xiao**[3], and **Jianjie Ma**[1,2,*]

[1]Department of Physiology and Biophysics, Robert Wood Johnson Medical School, Piscataway, NJ 08854

[2]Protein Therapy Division, TRIM-edicine, Inc, North Brunswick, NJ 08902

[3]Institute of Molecular Medicine, Peking University, Beijing, China

[4]Department of Biological Chemistry, Kyoto University Graduate School of Pharmaceutical Sciences, Kyoto, Japan

Abstract

Mitsugumin 53 (MG53), a muscle-specific TRIM family protein, is an essential component of the cell membrane repair machinery. Here we examined the translational value of targeting MG53 function in tissue repair and regenerative medicine. Although native MG53 protein is restricted to skeletal and cardiac muscle tissues, beneficial effects that protect against cellular injuries are present in non-muscle cells with overexpression of MG53. In addition to the intracellular action of MG53, injury to the cell membrane exposes a signal that can be detected by MG53, allowing recombinant MG53 protein to repair membrane damage when provided in the extracellular space. Recombinant human MG53 (rhMG53) protein purified from *Escherichia coli* fermentation provided dose-dependent protection against chemical, mechanical, or UV-induced damage to both muscle and non-muscle cells. Injection of rhMG53 through multiple routes decreased muscle pathology in the *mdx* dystrophic mouse model. Our data support the concept of targeted cell membrane repair in regenerative medicine, and present MG53 protein as an attractive biological reagent for restoration of membrane repair defects in human diseases.

Introduction

An emerging concept in recent biomedical research establishes that intrinsic membrane repair is a fundamental aspect of normal physiology and that disruption of this repair function underlies the progression of many human diseases (1-4). Plasma membrane repair is a highly conserved mechanism that appears in many eukaryotic cells (5-7). Although a

*Address correspondence to: noah.weisleder@umdnj.edu (N.W.); maj2@umdnj.edu (J.M.).

Author contributions: N.W., X.W., and J.M. developed the concept for the studies. N.W. and J.M. designed the experiments. N.T., P.L., T.T., C.F., R.Y., P.-J.C., X.Z., and M.H. participated in production of recombinant MG53 proteins. N.W., N.T., C.F., and P.J.C. developed methods to measure rhMG53 in cell based assays. N.T., X.W., C. Cao, Y.Z., P.L., H.Z., P.-J.C., M.S., C. Cai, H.C., H.T., and R.X. performed in vitro assays of MG53 function. N.W., N.T., T.T., C.F., H.Z., RY., X.Z., and H.T. performed in vivo assays. N.T., T.T. and R.Y. performed the toxicological assessments. N.W. and J.M. wrote the manuscript.

Competing interests: N.W. and J.M. have an equity interest in TRIM-edicine, which develops rhMG53 for treatment of human diseases. Patents on the use of rhMG53 are held by the University of Medicine and Dentistry of New Jersey (UMDNJ).

Data and materials availability: Access to rhMG53 protein can be obtained from TRIM-edicine, Inc. following establishment of a Material Transfer Agreement.

simple lipid bilayer membrane can reseal through thermodynamic principles, the presence of a cytoskeleton results in the plasma membrane being held under some degree of tension. When it is held under tension, small disruptions of the cell membrane cannot spontaneously reseal (8); thus, intracellular resealing mechanisms must exist. Compromised function in these repair mechanisms have been linked to muscular dystrophy (9-12), cardiovascular disease (13, 14), neurodegeneration (15), airway disorders (16), and other disease states in humans and in animal models. Targeting this conserved pathway as a therapeutic approach has proven difficult owing to limited knowledge of the molecular composition for the cell membrane repair machinery.

Recent advances have identified some components of the cell membrane repair process, particularly those involved in a putative pathway specific to striated muscles (2, 17), such as dysferlin (9, 14) and MG53 (18, 19). MG53 is a tripartite motif (TRIM) family protein (TRIM72) found principally in striated muscles, which plays an essential role in protection of skeletal and cardiac muscle cells against various types of acute injury or chronic physiological stresses. MG53 ablation results in defective sarcolemmal membrane repair with progressive muscle pathology (19, 20) and increased vulnerability of the heart to exercise stress and ischemia-reperfusion induced injury (18, 21).

Duchenne muscular dystrophy (DMD) is an X-linked inherited, progressive muscle wasting disorder that leads to compromised muscle structure, decreased muscle function, loss of independence and death near the second decade of life in affected males. DMD is the most prevalent form of muscular dystrophy with one in approximately 3300 live male births affected, making it the most common lethal genetic disease as nearly 20,000 children worldwide are born with DMD annually (22). In DMD, mutations in the dystrophin gene lead to a loss of protein expression that result in compromised sarcolemmal membrane integrity and extensive death of muscle fibers(23, 24).

DMD and other muscular dystrophies represent a truly unmet medical need as there is currently no cure for any form of muscular dystrophy. Current treatments center on preventing or reducing the resulting deformities in the joints and spine to allow people with DMD to remain mobile as long as possible. However, none of these treatments have any efficacy on the underlying pathology. Possible future therapies for DMD (25), including gene therapy replacement of dystrophin (26-28), myoblast treatment (29), and the use of stem cells (30, 31), hold promise and may eventually lead to effective treatments; however, these treatments are still years if not decades away from application in human patients. As a result, there is a great need for intermediate therapies to reduce the pathology associated with DMD and other muscular dystrophies to fill this unmet medical need.

In this study, we explore the therapeutic value for targeting MG53 function in tissue repair and regenerative medicine, specifically for the treatment of muscle damage and degeneration in DMD. We found that MG53 protein present in the serum can potentially be used as a biomarker for tissue injury, and that increased levels of recombinant MG53 protein in the extracellular solution could provide dose-dependent protection against injuries to both muscle and non-muscle cells. We also show that recombinant human MG53 protein can protect against tissue damage in skeletal muscle and can minimize the pathology associated with muscular dystrophy in the *mdx* mouse model.

Results

MG53 can increase membrane resealing in multiple cell types

MG53 is highly enriched in striated muscles, but it may also accelerate the conserved cell membrane repair mechanisms in non-muscle cells to provide beneficial health effects on the

targeted tissues. When a green fluorescent protein was fused to the amino-terminus of MG53 and heterologously expressed in several non-muscle cell types, confocal microscopy revealed rapid translocation of GFP-MG53 toward cell membrane injury sites that were caused by either physical penetration of a microelectrode (Fig. 1A) or permeabilization with saponin (Fig. 1B). Translocation of MG53 to sites of membrane injury in non-muscle cells, including epithelial, neuronal and immune origin cells, is similar to the response in skeletal and cardiac muscles (18-21), suggesting that MG53 may have broad therapeutic potential in both muscle and non-muscle tissues.

Although MG53 is an intracellular protein, native MG53 could be detected in the circulating blood of wild-type mice (Fig. 2A, B). Injury of the sarcolemmal membrane associated with contraction of the heart and skeletal muscles during 30 minutes of eccentric treadmill (running) exercise likely caused additional leakage of MG53 to the extracellular medium in wild-type mice. Compared to wild-type mice, high serum MG53 levels appeared in *mdx* mice in the resting state, because mice displaying a muscular dystrophy phenotype have fragile sarcolemmal membranes owing to the absence of dystrophin (32). Muscle membrane damage induced by eccentric contraction during downhill treadmill running increased MG53 levels in the serum of the *mdx* mice (Fig. 2A, B). The increase of native MG53 in the circulating blood of *mdx* mice may provide a quantitative biomarker for the diagnosis of muscle and heart pathology, and presents an opportunity to therapeutically target the extracellular population of MG53 to repair membrane defects.

We discovered that providing additional soluble MG53 protein to the extracellular space could increase the capacity of plasma membranes to reseal following acute injury. Isolated red fluorescent protein (RFP)-labeled MG53 was applied to the media surrounding cultured mouse C2C12 myotubes, before cells were mechanically wounded by penetration of a microelectrode through the cell membrane. As shown in Figure 2C and movie S1, accumulation of RFP-MG53 was observed at the extracellular injury sites following mechanical wounding of the C2C12 cells, indicating that externally applied MG53 protein can localize to sites of cell membrane disruption.

Extracellular MG53 protein increases membrane repair capacity in isolated cells

The primary amino acid sequence of MG53 does not contain consensus glycosylation sites or indications of other post-translational modifications. Therefore, *Escherichia coli* can be used to produce recombinant human MG53 protein (rhMG53). Expression of human MG53 linked to a polyhistidine (His-MG53) immunoaffinity tag (Fig. 2D) or maltose binding protein tag (MBP-MG53) in *E. coli* produced soluble protein that could be effectively isolated by affinity high-performance liquid chromatography (HPLC) (fig. S1A, C). A thrombin protease site was engineered between MBP and MG53 (fig. S1B) to allow for cleavage of MBP to generate the untagged rhMG53 protein (fig. S1E). This purified rhMG53 protein, with greater than 97% purity based on HPLC, could be lyophilized for long-term storage and remained soluble and functional upon reconstitution into physiological saline solutions. Additional protein isolation efforts show that functional rhMG53 can also be isolated from insect (Sf9) or mammalian (CHO) cells (fig. S1D, F). The latter is important because a common methodology for scaling up production of biologic drugs is secretion of the proteins from genetically modified CHO cells as an alternative to *E. coli* that can avoid potential issues with the removal of endotoxin during protein purification.

For quantification of the protective effect of rhMG53 in membrane damage, we adapted an assay to determine the amount of membrane damage produced in a large population of cells (33, 34). In this assay, we measured the quantity of an intracellular enzyme, lactate dehydrogenase (LDH), which leaks from the cell interior into the extracellular solution

following injury to the cell membrane. Using this assay, we found that HEK293 cells transfected with RFP-MG53 showed significantly reduced amount of LDH following electroporation-induced membrane damage (Fig. 2D), confirming that internal MG53 can function in membrane repair in non-muscle cells both by translocating to injury sites in non-muscle cells (Fig. 1) and also increasing membrane resealing capacity. Application of His-MG53 or rhMG53 protein to the extracellular media rather than transfection also reduced the amount of membrane damage resulting from two different damage paradigms, electroporation (Fig. 2E) and mechanical damage by glass micro-beads (Fig. 2F). This response was dose-dependent and could be eliminated by boiling the rhMG53 before application to the cells (Fig. 2F), indicating that properly folded rhMG53 is responsible for the increased membrane resealing. Aggregation of boiled rhMG53 resulted in scattering of light in this colormetric LDH assay and increased variability in these measurements. The protein tag appears to have no effect on MG53 function as both MBP-MG53 and rhMG53 proved to be equally effective at resealing the membrane of injured muscle cells *in vivo* (fig. 2G).

Several previous studies have established that long chain polymers, such as poloxomer 188 (P188) could increase membrane resealing in striated muscles (35-39), lung epithelium (16) and neurons (40-42), supporting the concept that modulation of membrane repair could have potential therapeutic value for human diseases. We compared the membrane repair function of rhMG53 and P188, and found that 300 nM rhMG53 could produce robust protection against mechanical damage to cells (Fig. 2H); whereas a 1000-fold greater concentration of P188 was needed to produce the same degree of membrane protection.

Extracellular MG53 protein increases membrane repair in muscle fibers

Further experiments were conducted to test if MG53 protein could prevent membrane damage in skeletal muscle fibers. A UV laser produced localized damage to the sarcolemmal membrane of isolated muscle fibers in the presence of a styrylpyridinium FM1-43 dye (9), which is non-fluorescent in aqueous solution but becomes intensely fluorescent when it enters the cell (7). Tracking the fluorescence allowed us to resolve the extent of membrane disruption. These tests showed that MBP-MG53 could increase membrane resealing in both *mg53*$^{-/-}$ (Fig. 3A) and *dysferlin*$^{-/-}$ (Fig. 3B) muscle fibers damaged by UV-laser, whereas bovine serum albumin (BSA), as a control protein, could not prevent FM1-43 dye entry. This indicates that MG53 can be effective in resealing the membrane of isolated muscle fibers with compromised membrane repair (9, 19). The striking protective effect of MBP-MG53 on UV-laser induced wound to isolated muscle fibers can be best appreciated in live cell images in movies S2 and S3. These results indicate that the extracellular mode of action of MG53 does not depend on the presence of native MG53 or dysferlin within the muscle fiber. Thus, it is possible that extracellular MG53 protein functions through a distinct mechanism that does not involve all the aspects of intracellular MG53 action, including interaction with dysferlin and differential regulation by the external oxidative state (19, 20).

MG53 can prevent muscle injury in vivo in mice

We next tested if MG53-mediated membrane repair could be applied to an *in vivo* model of cellular damage. To induce damage in native muscle, we injected cardiotoxin VII4 from *Naja mossambica* (CTX), a cytolytic toxin that disrupts cell membranes (43, 44), into the skeletal muscles of wild-type mice. Intramuscular (IM) co-injection of MBP-MG53 with CTX in the gastrocnemius significantly reduced the amount of toxin-induced muscle damage, as indicated by reduced release of LDH into the bloodstream after 16 hours (Fig. 4A). At 16 hours post-injection, the serum LDH levels have stabilized and can provide an effective marker of the damage of all cells at the injection site. Further studies showed that intravenous (IV) injection of MBP-MG53 prior to IM injection of CTX prevented release of

creatine kinase (CK) into the blood (Fig. 4B), indicating that MBP-MG53 delivered into the circulation could protect against localized injury to skeletal muscle. As a muscle-specific enzyme, CK levels provide a specific readout of disruption of striated muscle fiber membranes. Histological analysis showed that both IV and IM injections of MBP-MG53 could decrease the incidence of necrotic muscle fibers, fibrotic scarring, and lymphocyte infiltration compared to BSA (control) in muscles that were injured with CTX (Fig. 4C). Systemic IV delivery of rhMG53 could facilitate the treatment of DMD as the IM route would require multiple injections throughout the body. IV injection would also facilitate treatment of other systemic diseases.

We next used a dye exclusion assay to directly visualize the protective effect of MG53 on muscle membrane integrity *in vivo*. For these studies, membrane-impermeable Evans blue dye was co-injected with CTX and either MBP-MG53 or BSA into the wild-type mouse gastrocnemius muscles (Fig. 5A). Immunohistological staining showed muscle fibers that displayed MBP-MG53 on the plasma membrane showed less dye infiltration than those injected with BSA (Fig. 5B), illustrating that MG53 can directly influence the permeability of the cellular membrane. In some cells we observed MBP-MG53 inside the cell, suggesting some extracellular MBP-MG53 may enter the cell to facilitate membrane repair. However, because rhMG53 does not appear to require intracellular dysferlin to function (Fig. 3B), the mechanism of action of this exogenous protein is likely to have distinct aspects from the native MG53.

MG53 binds to phosphatidylserine to target areas of membrane disruption

The specificity of MG53 association with sites of membrane disruption requires recognition of lipid-based signals exposed at the extracellular space (45-47). Our previous findings showed that MG53 can specifically bind phosphatidylserine (PS) (19), a phospholipid usually sequestered on the inner leaflet of the plasma membrane that may be exposed to the extracellular environment following injury. To test whether the exposure of PS could provide a mechanism for MG53 tethering to the injury site, we co-injected MBP-MG53 or MBP-MBP (control) with CTX and a fluorescently labeled PS binding protein, FITC-Annexin V, into the gastrocnemius muscles of living mice. By injecting CTX to create membrane disruptions, we should expose PS to the extracellular space. The exposed PS could then be labeled by Annexin V and we could determine if the MBP-MG53 localized to the same sites of PS exposure. Annexin V appeared on the plasma membrane of damaged muscle fibers, and immunostaining for the exogenous MBP-MG53—but not MBP-MBP—revealed co-localization with Annexin V (Fig. 5C).

To further test if the association of PS with rhMG53 contributes to the observed increase in membrane repair, a series of competition experiments were conducted. Simultaneous treatment of cells with excess PS and rhMG53 could significantly reduce the membrane repair function of rhMG53 while phosphatidylcholine showed no significant effects on rhMG53 function (Fig. 5D). These results suggest that MG53 proteins bind exposed PS at sites of cell membrane disruption in order to facilitate membrane repair.

Recombinant MG53 can protect against damage in a mouse model of muscular dystrophy

Intrinsic membrane repair is a fundamental aspect of normal human physiology and disruption of this repair function underlies the progression of several pathologies (2, 4, 15, 17, 48), including DMD. DMD is a common genetic disease associated with defective skeletal muscle sarcolemmal membrane integrity (49-51), for which there are currently no approved drugs that target the underlying pathology. We investigated the ability of rhMG53, administered systemically, to prevent muscle damage in the *mdx* mouse model of DMD. We performed an initial study with IV injection of MBP-MG53 into adult *mdx* mice that were

subjected to downhill treadmill running to produce muscle membrane damage. These studies test another method of membrane disruption complementary to toxin-mediated injury (Fig. 3). Thirty minutes prior to downhill running, two groups of mice were injected with BSA (control) or MBP-MG53 (8 mg/kg). As shown in Figure 6A, *mdx* mice receiving tail vein injection of MG53 showed significantly reduced serum CK levels at 30 minutes post-running.

We next applied rhMG53 to *mdx* mice 4-5 weeks of age to target the first episode where significant myonecrosis and dystrophic symptoms of DMD begin to develop. In these experiments, 4 week old *mdx* mice were injected twice daily with rhMG53 (8 mg/kg) or saline vehicle control for four days. During this time, there was no difference in body weight increase between the rhMG53 and control groups (fig. S3), indicating that rhMG53 was well tolerated. After four days, these mice were assessed for improvement in skeletal muscle structure. We saw significant reductions in the extent of fibrosis (Fig. 6B) and the number of Evans blue dye–positive fibers (Fig. 6C, D) in *mdx* gastrocnemius and tibialis anterior (TA) skeletal muscles following a short treatment with rhMG53. Due to the variability in the extent of myonecrosis in *mdx* mice at this age, particularly within the TA, fibrosis measurements did not provide statistical significance in the TA. Improvement in muscle structure with rhMG53 application was also seen in *mdx* diaphragm muscle (Fig. 6D; fig. S4).

Although IV application of rhMG53 was effective at reducing muscle pathology in mdx mice, this mode of delivery is not optimal for the chronic treatment regimens necessary for DMD patients. Injection through a subcutaneous (SC) route would allow for simpler administration of each dose of rhMG53; thus, we tested if SC injection could deliver rhMG53 into the bloodstream of wild-type and *mdx* mice, and if this delivery method could prevent damage associated with exercise. SC injection of 8 mg/kg rhMG53 into mice showed that MG53 appeared in the bloodstream within 15 minutes of the injection and the serum level of MG53 reached a peak level at 4 hours after injection (Fig. 6E). Littermate *mdx* mice were injected SC with rhMG53 or saline vehicle 2 hours before running on a rodent treadmill, and serum CK levels were measured 30 minutes after the cessation of running. We found that rhMG53 could significantly decrease the amount of CK release into the blood following exercise (Fig. 6F). As expected, SC injection had similar effects in this assay as IV injection; however, we used a higher dose to compensate for the altered pharmacokinetics of rhMG53 following SC injections (Fig. 6E). Together, these studies establish that SC delivery of rhMG53 can provide therapeutic levels of active protein that can potentially prevent dystrophic pathology in *mdx* mice.

Pharmacokinetics and toxicity of MG53 in vivo

We performed Western blot and ELISA with serum samples obtained from mice following tail vein injection of MBP-MG53 in order to determine the pharmacokinetic properties of MG53. At six hours post-IV injection, approximately 20% of the initial dose of MBP-MG53 was present in the blood (fig. S5). This suggests that MBP-MG53 would be effective at providing protective effects against acute tissue injuries as the protein could be present during a window where cell death events were expected after an acute injury. However, longer term application may require additional protein engineering to extend the half life of the MG53 protein. In addition, we found that, with multiple IV injections of rhMG53 (twice daily for 4 days), there were no significant changes in the body weight (fig. S3) of the mice ($P > 0.05$), suggesting there is limited toxicology associated with injection of rhMG53. This was further tested by daily SC injection of rhMG53 for two weeks, which did not produce any observable toxic effects at the end of two weeks as measured by body weight**,** histopathology and serum biomarkers for liver function (alanine aminotransferase, LDH)

and inflammation (interleukin 6 and tumor necrosis factor α) (fig. 7). Only the terminal time point was measured, as any toxicity would be expected to accumulate over the course of the treatment and should be resolved at the end of the trial.

Discussion

The data presented here indicate that recombinant MG53 proteins can increase the capacity of different cell types to reseal membrane disruptions through a mechanism that appears to be distinct from that of native intracellular MG53. Our data suggest that rhMG53 could be a therapeutic agent for the treatment of DMD, and potentially other human diseases where membrane injuries contribute to the pathogenesis of the disorder. We show that recombinant MG53 proteins can identify external signals at membrane disruptions and increase membrane resealing in cultured muscle and non-muscle cells when applied to the extracellular solution. Animal studies with the *mdx* mouse provide evidence that application of rhMG53 through multiple routes (IM, IV, or SC) can improve the membrane repair capacity of skeletal muscle fibers, as well as ameliorate some of the pathology associated with muscular dystrophy.

One aspect of DMD pathophysiology is the fragility of the sarcolemmal membranes owing to the absence of dystrophin. Current therapeutic approaches under development generally focus on restoration of dystrophin expression through gene therapy (26-28) and pharmacological (52, 53) methods, regeneration of muscle fibers with cell-based therapy (29-31), or blocking calcium influx into dystrophic fibers (54). Because clinical applications of gene therapy or stem cell therapy are not likely to occur in the near future, protein therapeutic approaches, including rhMG53 and other proteins (55, 56), may prove to be useful for the treatment of DMD patients in the short term.

Several of our findings suggest that MG53 could be translated into a treatment for use in human patients to target cell membrane repair in regenerative medicine. We show that serum levels of MG53 could be used as a biomarker to detect physiological and pathophysiological changes in muscle structure, such as those associated with muscle injury or diseases of the striated muscles. Because the native MG53 protein is present in the circulating blood, the risk that systemic delivery of recombinant MG53 protein would produce immunogenic or toxicological effects is minimized. In all of our studies we used the human MG53 protein to establish the human sequence was successful at increasing membrane resealing. Furthermore, we found that MG53 can function in different human cell lines, suggesting that rhMG53 can increase membrane resealing in cells of human origin. Finally, the fact that rhMG53 protein can be effectively produced in microorganisms or mammalian cells that are widely used in bioprocess development also simplifies the translation of these findings into human patients.

One caveat on the use of the *mdx* mouse model in these studies is that the extent of pathology seen in these mice does not reach the severity seen in human DMD patients. Additional studies using more predictive models of DMD, including dystrophic dogs and cultured human dystrophic muscle cells, should help determine the extent that delivery of rhMG53 can have protective effect on damage to the dystrophic muscle. Another useful study will be to conduct longer term trials in these models to see if chronic degeneration can be targeted by rhMG53 to complement the treadmill and shorter term studies presented in the current study.

The extracellular activity of MG53 suggests that native MG53 in striated muscle released into the extracellular space may also participate in increasing local membrane resealing capacity. While the serum concentrations of MG53 appear to be below what would be

considered a therapeutic level in our assays, the levels of MG53 at the microdomain of a membrane disruption would be significantly higher. MG53 released thought a membrane disruption could feed back and increase membrane repair by interacting with PS exposed on the cell surface associated with membrane disruption, allowing for more cells to survive an insult and potentially reducing the extent of pro-inflammatory factors release to further improve the structure and functional capacity after injury of a target tissue. It is also possible that cholesterol could provide an additional lipid signal that could be exposed at the injury site, as our previous studies showed that intracellular MG53 function in cardiomyocytes involves interaction with cholesterol (18, 33). Another possibility is that the release of MG53 from striated muscle fibers could provide an endocrine signal that participates in additional protective responses in other cells or tissues. Further studies should establish additional details on the mechanisms contributing to the protective effects of MG53 protein, which will inform efforts to translate the findings presented here into effective treatments for human diseases linked to defective tissue repair and regeneration. Considering that breakdown of the plasma membrane is generally associated with necrotic cell death, MG53 may be an effective therapeutic approach for many human diseases where accidental necrotic cell death is an important pathologic component including myocardial infarction, neurodegeneration, pulmonary defects, and traumatic injuries to muscle and non-muscle tissues.

Materials and Methods

Cell culture, transfection, and microelectrode damage

Human embryonic kidney (HEK293), Chinese hamster ovary (CHO), human cervical epithelium (Hela), mouse myoblast (C2C12), mouse leukaemic macrophages (RAW 264.7), human embryonic palatial mesenchymal (HEPM), human bronchial epithelia (C38), human astrocyte (A735) and human gastric adenocarcinoma (AGS) cells were initially purchased from American Type Culture Collection (ATCC) and maintained per ATCC suggested protocols. Cells were transfected with GFP-MG53 or RFP-MG53 plasmids (19) using Genejammer transfections reagent (Stratagene/Agilent Technology) per manufacturer's suggested protocols. Adult human primary keratinocytes (Lonza) were infected with an adenovirus expressing GFP-MG53 by application of adenovirus at a multiplicity of infection (MOI) of 100 in serum-free Dulbecco's modified Eagle's medium as described previously (18). Cells were cultured on glass-bottomed deltaT dishes (Bioptechs) and imaged on a Radiance 2100 laser confocal scanning microscope (BioRad) with a 40× 1.3-NA oil immersion objective (Nikon). Microelectrodes were pulled from borosilicate capillaries (PYREX® Part No. 9530-2) and mounted on a three-axis micromanipulator (Narishige). The microelectrode tip was inserted into the cell membrane then rapidly removed while recording 512×512 pixel x-y scans of both bright field and GFP or RFP fluorescence at a rate of 3.08 seconds per image.

Purification of recombinant MG53 and Western blot

For protein amplification in *E. coli*, optimal protein expression level and prevention of degradation occur when the bacterial host strain M15 is grown for 4 hours at 16°C after induction with 1 mM IPTG. After incubation with 1 mg/ml lysozyme for 30 min and sonication, the *E. coli* lysate was solubilized with 1% digitonin for 30 min on ice and centrifuged at 200,000 × g for 30 min at 4°C. Fusion proteins were purified using either HisTrap FF or MBP Trap HP immunoaffinity columns (GE Biosciences) on an AKTAxpress high pressure liquid chromatography system (GE Biosciences). MBP-MG53 (1 mg/ml) was digested by 10 U/mL bovine thrombin (BioPharm Laboratories) in 10 ml digestion buffer containing 25 mM TrisCl, pH 7.5, 154 mM NaCl, and 0.5 mM dithiothreitol

(Sigma) for 2 h at 25°C. rhMG53 was isolated by two additional passes through a MBP Trap HP column and protein concentration was measured using the DC protein assay (BioRad).

To isolate RFP-MG53 protein from HEK293 cells, approximately 4×10^6 cells were transfected with RFP-MG53 and then cultured for 24 hours before cells were harvested by trypsinization, washed and resuspended in phosphate buffered saline (PBS) then lysed using three cycles of freezing and thawing. The lysate was cleared by centrifugation (5000 × g for 10 min) and then directly applied to the cells before microelectrode wounding. His-MG53 and MBP-MG53 plasmids were generated by PCR amplification cloning the human MG53/TRIM72 cDNA (Genbank NM_001008274) into the pGene/V5-His (Invitrogen) or pMAL-P2 (New England Biolabs) vectors, respectively, to fuse the immunoaffinity tag to the N-termius of the MG53 protein. A thrombin protease site was inserted into the PCR primer between MG53 cDNA and the immunoaffinity tag to allow for later cleavage of the tag from the rhMG53 protein. The pSecTag2/Hygro plasmid system (Invitrogen) was used to generate MG53 secretion per manufacturer's directions.

SDS-PAGE gels loaded with the designated amount of protein were either stained with Coomassie Brilliant Blue or transferred onto polyvinylidene fluoride membranes (BioRad). Western blotting was conducted using an ECL+ kit (GE Biosciences) per manufacturer's instructions using custom rabbit polyclonal anti-MG53 (19) (1:1000 dilution), mouse monoclonal anti-MBP (NEB Biolabs, 1:2000 dilution) or mouse monoclonal anti-myc (Sigma, 1:2000 dilution) as a primary antibody and the appropriate secondary antibody coupled to HRP (Sigma, 1:5000 dilution). The resulting x-ray films were scanned and then analyzed for band intensity using ImageJ software (National Institutes of Health).

Mouse models of muscle membrane damage

Male C57BL/10ScSn-*Dmd*^{mdx}/J (*mdx*) or C57BL/10ScSnJ mice were purchased (Jackson Laboratories). C57bl6/J mice were bred at the Vivarium at Robert Wood Johnson Medical School. All animals were treated in accordance with institutional guidelines with IACUC approved protocols. At 4-5 months of age, *mdx* and C57BL/10ScSnJ control mice were treated with 10 μM cardiotoxin VII4 (CTX, Sigma-Aldrich) or exercised on an Exer 3/6 rodent treadmill (Columbus Instruments) at a 15° down angle for 90 min at 10 m/min. Following CTX injection or exercise, approximately 10 μL of serum was used to measure creatine kinase levels with a CK-MB kit (Genzyme Diagnostics) per manufacturer's instructions. C57bl6/J mice were anesthetized with isoflurane and then injected using 22.5 gauge hypodermic needles with a mixture of reagents as described with IV injections conducted through the caudal vein and blood collections made through cheek punch using Goldenrod Animal Bleeding Lancet (Medipoint). Commercial enzyme activity kits were used to measure LDH (Clontech Laboratories) and CK levels (Genzyme Diagnostics) using a Flexstation3 pate reader (Molecular Devices) per manufacturer's directions. Toxicological assessment was conducted using twice daily SC injection of rhMG53 (8 mg/kg) into *mdx* mice. After 14 days, mice were weighed and serum was collected via cardiac puncture for ELISA tests for the levels of TNFα (Invitrogen), IL-6 (Invitrogen) and alanine aminotransferase (NovaTein Biosciences). For all histological analyses, the listed tissues were surgically dissected, fixed in formalin (Electron Microscopy Services) overnight at 4°C, and either used for frozen sections or processed for histology by the Tissue Analytic Service at the Cancer Institute of New Jersey.

Cell models of membrane damage

HEK293 cells (9×10^4 cells per well) were suspended in 150 μl of D-PBS (Invitrogen) in the presence and absence of acid-washed beads (Sigma, 20 mg) and indicated doses of recombinant proteins or BSA per well of a 96 well-plate. The plate was shaken at 180 rpm

for 6 min at room temperature on an orbital shaker (Belloco Biotechnology). The 96-well plate was then centrifuged to remove cells and glass beads (2000 × g for 10 min). For electroporation-based damage, HEK293 (2×10^5) or C2C12 (1×10^5) cells were resuspended in 60 μL siPORTER electropration buffer and electroporated at indicated voltages in the siPORTER electroportation chamber per manufacturer's directions (Ambion). After shaking, the 96-well plate was centrifuged at 1000 × g for 10 min and 50 μL of the supernatant was transferred to a new 96-well plate for measuring LDH levels. LDH activity was determined using a colormetric kit (BioVision) on a SpectraFluor Plus plate reader (Tecan) per manufacturer's directions.

Muscle fiber model of membrane damage

Flexor digitorum brevis (FDB) muscle fibers were isolated by enzymatic digestion and tested for membrane repair capacity by measuring entry of FM1-43 styrylpyridinium dye (Invitrogen) following UV laser damage, as previously described (9, 19). Briefly, FDB muscles were digested in type II collagenase (Sigma) for approximately 60 min before isolation using pipette titration. Isolated fibers were plated on deltaT dishes and FM1-43 dye (2.5 μM) was added. Fibers were imaged on a LSM 510 confocal microscope (Zeiss) and an area of approximately 0.9 μm × 0.9 μm of the plasma membrane was irradiated using a UV laser (80 mW) set to maximum power for 5 seconds. Images were captured at intervals of 5 seconds each for up to 5 minutes. The resulting data was analyzed by calculating the change in fluorescence intensity ($\Delta F/F_0$) between each captured frame using ImageJ software.

Statistical analysis

Analysis of Variance (ANOVA) and *t*-test parametric analysis were used to determine statistical significance as described in individual figure legends. A threshold of $P < 0.05$ was used for statistical significance in most conditions, except where otherwise noted. Statistical testing was performed using Prism software (GraphPad).

Supplementary Material

Refer to Web version on PubMed Central for supplementary material.

Acknowledgments

We thank Zelgen-Biopharm for their assistance in developing methodology for the scale-up production of recombinant MG53 proteins.

Funding: This work was supported by grants from the National Institutes of Health to N.W. (AR063084) and J.M. (AG015556, HL069000, AR061385), a developmental grant from the Jain Foundation and a NIH SBIR grant (AR060019) to TRIM-edicine, and the Tissue Analytic Services Shared Resource of The Cancer Institute of New Jersey (P30CA072720).

References and Notes

1. McNeil PL, Steinhardt RA. Plasma membrane disruption: repair, prevention, adaptation. Annu Rev Cell Dev Biol. 2003; 19:697–731. [PubMed: 14570587]
2. McNeil PL, Kirchhausen T. An emergency response team for membrane repair. Nat Rev Mol Cell Biol. Jun.2005 6:499–505. [PubMed: 15928713]
3. Steinhardt RA, Bi G, Alderton JM. Cell membrane resealing by a vesicular mechanism similar to neurotransmitter release. Science. Jan 21.1994 263:390–3. [PubMed: 7904084]
4. McNeil PL, Ito S. Gastrointestinal cell plasma membrane wounding and resealing in vivo. Gastroenterology. May.1989 96:1238–48. [PubMed: 2703112]
5. McNeil PL, Khakee R. Disruptions of muscle fiber plasma membranes. Role in exercise-induced damage. Am J Pathol. May.1992 140:1097–109. [PubMed: 1374591]

6. Clarke MS, Caldwell RW, Chiao H, Miyake K, McNeil PL. Contraction-induced cell wounding and release of fibroblast growth factor in heart. Circ Res. Jun.1995 76:927–34. [PubMed: 7538917]
7. Miyake K, McNeil PL. Vesicle accumulation and exocytosis at sites of plasma membrane disruption. J Cell Biol. Dec.1995 131:1737–45. [PubMed: 8557741]
8. Togo T, Krasieva TB, Steinhardt RA. A decrease in membrane tension precedes successful cell-membrane repair. Mol Biol Cell. Dec.2000 11:4339–46. [PubMed: 11102527]
9. Bansal D, et al. Defective membrane repair in dysferlin-deficient muscular dystrophy. Nature. May 8.2003 423:168–72. [PubMed: 12736685]
10. van der Kooi AJ, et al. Limb-girdle muscular dystrophy in the Netherlands: gene defect identified in half the families. Neurology. Jun 12.2007 68:2125–8. [PubMed: 17562833]
11. Jaiswal JK, et al. Patients with a non-dysferlin Miyoshi myopathy have a novel membrane repair defect. Traffic. Jan.2007 8:77–88. [PubMed: 17132147]
12. Cooper ST, et al. Dystrophinopathy carrier determination and detection of protein deficiencies in muscular dystrophy using lentiviral MyoD-forced myogenesis. Neuromuscul Disord. Apr.2007 17:276–84. [PubMed: 17303423]
13. Wenzel K, et al. Dysfunction of dysferlin-deficient hearts. J Mol Med. Nov.2007 85:1203–14. [PubMed: 17828519]
14. Chase TH, Cox GA, Burzenski L, Foreman O, Shultz LD. Dysferlin deficiency and the development of cardiomyopathy in a mouse model of limb-girdle muscular dystrophy 2B. Am J Pathol. Dec.2009 175:2299–308. [PubMed: 19875504]
15. Bazan NG, Marcheselli VL, Cole-Edwards K. Brain response to injury and neurodegeneration: endogenous neuroprotective signaling. Ann N Y Acad Sci. Aug.2005 1053:137–47. [PubMed: 16179516]
16. Gajic O, et al. Ventilator-induced cell wounding and repair in the intact lung. Am J Respir Crit Care Med. Apr 15.2003 167:1057–63. [PubMed: 12480613]
17. Doherty KR, McNally EM. Repairing the tears: dysferlin in muscle membrane repair. Trends Mol Med. Aug.2003 9:327–30. [PubMed: 12928033]
18. Wang X, et al. Cardioprotection of ischemia/reperfusion injury by cholesterol-dependent MG53-mediated membrane repair. Circ Res. Jul 9.2010 107:76–83. [PubMed: 20466981]
19. Cai C, et al. MG53 nucleates assembly of cell membrane repair machinery. Nat Cell Biol. Jan.2009 11:56–64. [PubMed: 19043407]
20. Cai C, et al. Membrane repair defects in muscular dystrophy are linked to altered interaction between MG53, caveolin-3, and dysferlin. J Biol Chem. Jun 5.2009 284:15894–902. [PubMed: 19380584]
21. Cao CM, et al. MG53 constitutes a primary determinant of cardiac ischemic preconditioning. Circulation. Jun 15.2010 121:2565–74. [PubMed: 20516375]
22. Moser H. Duchenne muscular dystrophy: pathogenetic aspects and genetic prevention. Hum Genet. 1984; 66:17–40. [PubMed: 6365739]
23. Ray PN, et al. Cloning of the breakpoint of an X;21 translocation associated with Duchenne muscular dystrophy. Nature. 318:672–5. Dec 19-1986 Jan 1, 1985. [PubMed: 3001530]
24. Campbell KP. Three muscular dystrophies: loss of cytoskeleton-extracellular matrix linkage. Cell. Mar 10.1995 80:675–9. [PubMed: 7889563]
25. Partridge TA. Impending therapies for Duchenne muscular dystrophy. Curr Opin Neurol. Oct. 24:415–22. [PubMed: 21892079]
26. Watchko J, et al. Adeno-associated virus vector-mediated minidystrophin gene therapy improves dystrophic muscle contractile function in mdx mice. Hum Gene Ther. Aug 10.2002 13:1451–60. [PubMed: 12215266]
27. Yanagihara I, et al. Expression of full-length human dystrophin cDNA in mdx mouse muscle by HVJ-liposome injection. Gene Ther. Jun.1996 3:549–53. [PubMed: 8789805]
28. Clemens PR, et al. In vivo muscle gene transfer of full-length dystrophin with an adenoviral vector that lacks all viral genes. Gene Ther. Nov.1996 3:965–72. [PubMed: 8940636]
29. Gussoni E, et al. Normal dystrophin transcripts detected in Duchenne muscular dystrophy patients after myoblast transplantation. Nature. Apr 2.1992 356:435–8. [PubMed: 1557125]

30. Gussoni E, et al. Dystrophin expression in the mdx mouse restored by stem cell transplantation. Nature. Sep 23.1999 401:390–4. [PubMed: 10517639]
31. Sampaolesi M, et al. Mesoangioblast stem cells ameliorate muscle function in dystrophic dogs. Nature. Nov 30.2006 444:574–9. [PubMed: 17108972]
32. Nonaka I. Animal models of muscular dystrophies. Lab Anim Sci. Feb.1998 48:8–17. [PubMed: 9517883]
33. Zhu H, et al. Polymerase transcriptase release factor (PTRF) anchors MG53 protein to cell injury site for initiation of membrane repair. J Biol Chem. Apr 15.2011 286:12820–4. [PubMed: 21343302]
34. Lin P, et al. Nonmuscle myosin IIA facilitates vesicle trafficking for MG53-mediated cell membrane repair. Faseb J. Jan 17.2012
35. Ng R, Metzger JM, Claflin DR, Faulkner JA. Poloxamer 188 reduces the contraction-induced force decline in lumbrical muscles from mdx mice. Am J Physiol Cell Physiol. Jul.2008 295:C146–50. [PubMed: 18495816]
36. Greenebaum B, et al. Poloxamer 188 prevents acute necrosis of adult skeletal muscle cells following high-dose irradiation. Burns. Sep.2004 30:539–47. [PubMed: 15302418]
37. Lee RC, River LP, Pan FS, Ji L, Wollmann RL. Surfactant-induced sealing of electropermeabilized skeletal muscle membranes in vivo. Proc Natl Acad Sci U S A. May 15.1992 89:4524–8. [PubMed: 1584787]
38. Townsend D, et al. Chronic administration of membrane sealant prevents severe cardiac injury and ventricular dilatation in dystrophic dogs. J Clin Invest. Apr 1.2010 120:1140–50. [PubMed: 20234088]
39. Yasuda S, et al. Dystrophic heart failure blocked by membrane sealant poloxamer. Nature. Aug 18.2005 436:1025–9. [PubMed: 16025101]
40. Follis F, et al. Role of poloxamer 188 during recovery from ischemic spinal cord injury: a preliminary study. J Invest Surg. Mar-Apr;1996 9:149–56. [PubMed: 8725553]
41. Frim DM, et al. The surfactant poloxamer-188 protects against glutamate toxicity in the rat brain. Neuroreport. Jan 19.2004 15:171–4. [PubMed: 15106852]
42. Kilinc D, Gallo G, Barbee K. Poloxamer 188 reduces axonal beading following mechanical trauma to cultured neurons. Conf Proc IEEE Eng Med Biol Soc. 2007; 2007:5395–8. [PubMed: 18003228]
43. Gulik-Krzywicki T, Balerna M, Vincent JP, Lazdunski M. Freeze-fracture study of cardiotoxin action on axonal membrane and axonal membrane lipid vesicles. Biochim Biophys Acta. Apr 22.1981 643:101–14. [PubMed: 7236681]
44. Rivas EA, Le Maire M, Gulik-Krzywicki T. Isolation of rhodopsin by the combined action of cardiotoxin and phospholipase A2 on rod outer segment membranes. Biochim Biophys Acta. Jun 9.1981 644:127–33. [PubMed: 7260064]
45. Dressler V, Schwister K, Haest CW, Deuticke B. Dielectric breakdown of the erythrocyte membrane enhances transbilayer mobility of phospholipids. Biochim Biophys Acta. Jul 13.1983 732:304–7. [PubMed: 6871195]
46. Fujiwara T, Ritchie K, Murakoshi H, Jacobson K, Kusumi A. Phospholipids undergo hop diffusion in compartmentalized cell membrane. J Cell Biol. Jun 10.2002 157:1071–81. [PubMed: 12058021]
47. Sonnleitner A, Schutz GJ, Schmidt T. Free Brownian motion of individual lipid molecules in biomembranes. Biophys J. Nov.1999 77:2638–42. [PubMed: 10545363]
48. Bansal D, Campbell KP. Dysferlin and the plasma membrane repair in muscular dystrophy. Trends Cell Biol. Apr.2004 14:206–13. [PubMed: 15066638]
49. Fong PY, Turner PR, Denetclaw WF, Steinhardt RA. Increased activity of calcium leak channels in myotubes of Duchenne human and mdx mouse origin. Science. Nov 2.1990 250:673–6. [PubMed: 2173137]
50. Deconinck N, Dan B. Pathophysiology of duchenne muscular dystrophy: current hypotheses. Pediatr Neurol. Jan.2007 36:1–7. [PubMed: 17162189]
51. Pasternak C, Wong S, Elson EL. Mechanical function of dystrophin in muscle cells. J Cell Biol. Feb.1995 128:355–61. [PubMed: 7844149]

52. Yokota T, et al. Efficacy of systemic morpholino exon-skipping in Duchenne dystrophy dogs. Ann Neurol. Jun.2009 65:667–76. [PubMed: 19288467]

53. Welch EM, et al. PTC124 targets genetic disorders caused by nonsense mutations. Nature. May 3.2007 447:87–91. [PubMed: 17450125]

54. Allen DG, Whitehead NP. Duchenne muscular dystrophy--what causes the increased membrane permeability in skeletal muscle? Int J Biochem Cell Biol. Mar.2011 43:290–4. [PubMed: 21084059]

55. Rooney JE, Gurpur PB, Burkin DJ. Laminin-111 protein therapy prevents muscle disease in the mdx mouse model for Duchenne muscular dystrophy. Proc Natl Acad Sci U S A. May 12.2009 106:7991–6. [PubMed: 19416897]

56. Sonnemann KJ, et al. Functional substitution by TAT-utrophin in dystrophin-deficient mice. PLoS Med. May 26.2009 6:e1000083. [PubMed: 19478831]

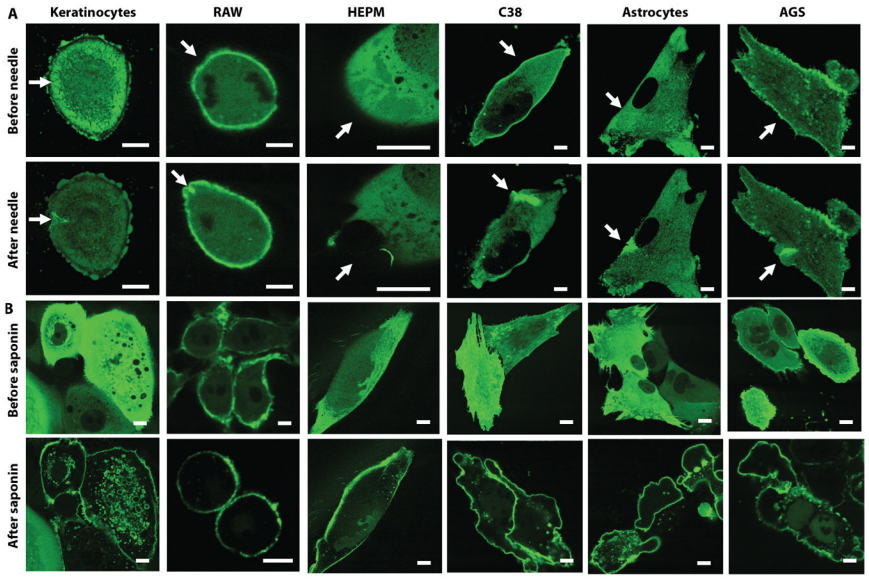

Figure 1. MG53 functions in membrane repair in non-muscle cell types

Various cultured cell types were transfected with GFP-MG53, including human gastic epithelium (AGS), airway epithelium (C38), human embryonic palatal mesenchyma (HEPM) cells, primary adult keratinocytes, mouse neuronal (astrocytes), and mouse immune (RAW) cells. Fluorescence shows localization of MG53 to the membrane upon injury. Scale bars, 2 μm. (**A**) Cells were subjected to mechanical membrane damage by microelectrode needle penetration (arrow points to location of injury). (**B**) The membranes of cells were permeabilized using saponin detergent (0.001% in saline).

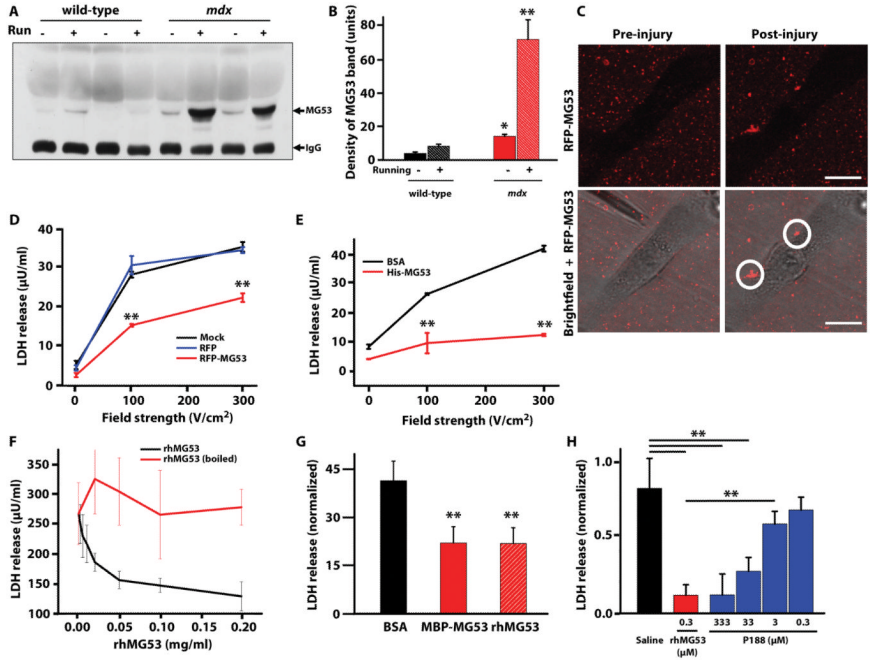

Figure 2. Recombinant MG53 applied exogenously can identify sites of membrane disruption and translocate to injury sites

(**A**) Western blots of MG53 in purified mouse serum samples (n = 8 mice per group) of both wild-type and *mdx* dystrophic mice at the resting state (−) and with 30 minutes of treadmill exercise ("running", +). (**B**) Densitometry analysis of (A). *P < 0.05, **P < 0.01 versus respective wt control by ANOVA. (**C**) Microsomal membrane vesicles were isolated from HEK293 cells transiently transfected with RFP-MG53. Vesicles containing RFP-MG53 were applied to the culture medium of C2C12 myotubes prior to injury with a microelectrode, and localization of RFP-MG53 was observed by confocal (left) and bright field microscopy (right). RFP-MG53 translocation to sites of membrane damage is marked by white circles. Lve cell imaging of this assay is provided (movie S1). Scale bars, 10 μm. (**D**) HEK293 cells transfected with RFP-MG53, RFP, or mock (transfection reagent only) conditions were exposed to a single square wave electric pulse of varying field strengths to electroporate the cell membrane. Levels of LDH released into the surrounding media were determined for 2×10^5 cells per well. Data are means ± SD (n=4). **P < 0.01 compared to RFP by ANOVA. (**E**) Soluble His-MG53 can prevent damage by various strength electric fields in HEK293 cells. Cells were pre-treated with either 30 μg/mL of either MG53 or BSA. Data are means ± SD (n=6). **P < 0.01, ANOVA. (**F**) HEK293 cells were incubated with various doses of rhMG53 or boiled rhMG53 before mechanical membrane damage by glass microbeads. Data are means ± SD (n=6). ANOVA established statistical significance (P<0.05) at concentrations higher than 0.0125 mg/ml. (**G**) Serum creatine kinase (CK) levels in wild-type mice injected intravenously with equimolar quantities of BSA, MBP-MBP, or rhMG53 followed by IM injection of cardiotoxin into the gastrocnemius. Data is presented as the fold increase over the basal CK levels. Data are mean fold increase over basal CK levels ± SD (n=6 mice per treatment group). **P < 0.01 versus BSA, control by ANOVA. (H) LDH release following glass microbead wounding of HEK293 cells in the presence of saline vehicle, rhMG53, or Poloxamer 188 (P188) at various concentrations. Data are normalized to the values from saline-treated samples to avoid interference at high P188 concentrations. Data are means ± SEM (n=6), **P < 0.01 versus indicated group by ANOVA.

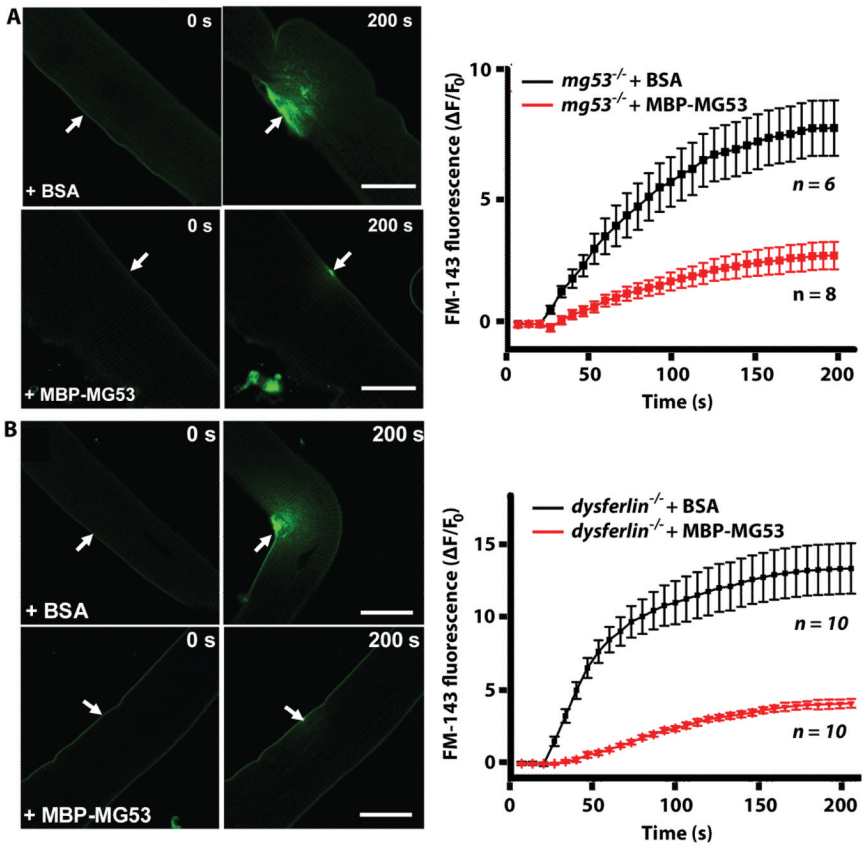

Figure 3. Application of soluble rhMG53 increases membrane repair capacity *in vitro*

(**A**) Isolated flexor digitorum brevis (FDB) muscle fibers from *mg53*$^{-/-}$ mice were treated with FM1-43 dye and 80 μg/mL MBP-MG53 or BSA, before injury by a UV laser (arrow). Scale bars, 20 μm. Degree of dye influx in multiple fibers is quantified as the change in fluorescent signal over baseline ($\Delta F/F_0$). Data are means ± SD (*n* represents individual muscle fibers). (**B**) Isolated FDB muscle fibers from *dysferlin*$^{-/-}$ mice were treated with 80 μg/ml MBP-MG53 or BSA before injury by a UV laser (arrow). Scale bars, 20 μm. Fluorescence influx data ($\Delta F/F_0$) for multiple fibers are shown on the right. Data are averages ± SD (n represents individual muscle fibers). Live imaging of this assay (movies S2 and S3) show entire time course of fluorescence influx after injury, from 0 to 200 seconds.

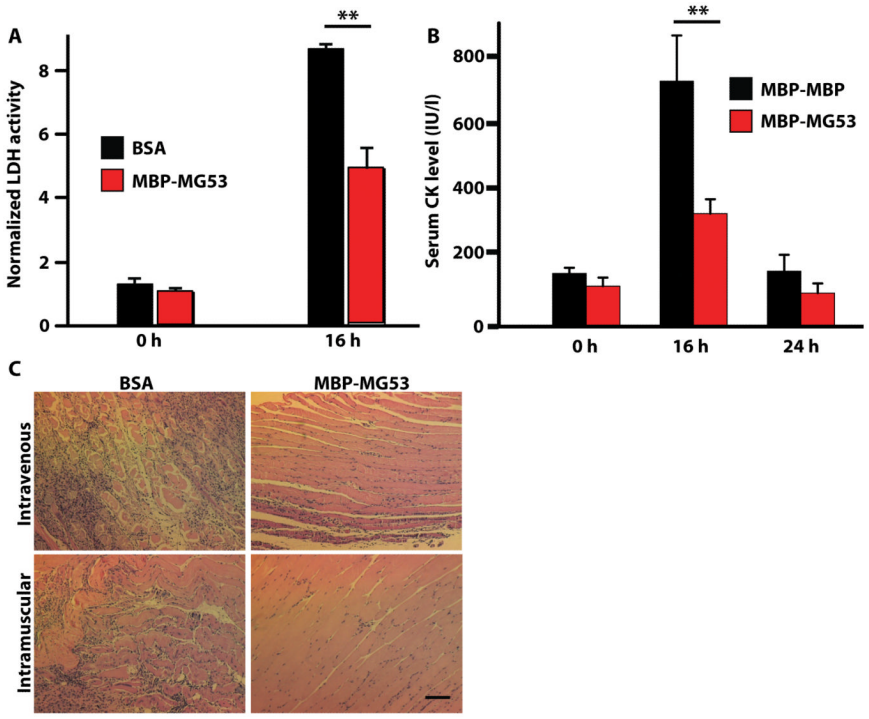

Figure 4. MG53 protein protects against muscle damage in vivo

(**A**) Serum LDH levels for wild-type mice co-injected in the gastrocnemius muscle with CTX (10 μM) and either rhMG53 (20 μg/mL) or BSA. Before toxin injection is $t = 0$ hours. Data are normalized to $t = 0$ for each group and presented as means ± SD (n=6-8 mice per treatment group). $^{**}P < 0.01$, ANOVA. (**B**) Serum creatine kinase (CK) levels in wild-type mice injected intravenously with rhMG53 or MBP-MBP, a control protein containing a tandem MBP tag, followed by IM injection of CTX into the gastrocnemius. Data are means ± SD (n=6 mice per treatment group). $^{**}P < 0.01$ versus MBP-MBP control at that time point, ANOVA. (**C**) Histological sections of gastrocnemius muscle. In the top row, mice were first injected intravenously with BSA or MBP-MG53 before intramuscular injection of CTX (10 μM). In the bottom row, mice were simultaneously injected intramuscularly with CTX and either BSA or MBP-MG53. Tissues were collected at 7 days after injections. Images are representative of ≥12 fields examined from 4-6 mice per condition. Scale bar, 50 μm.

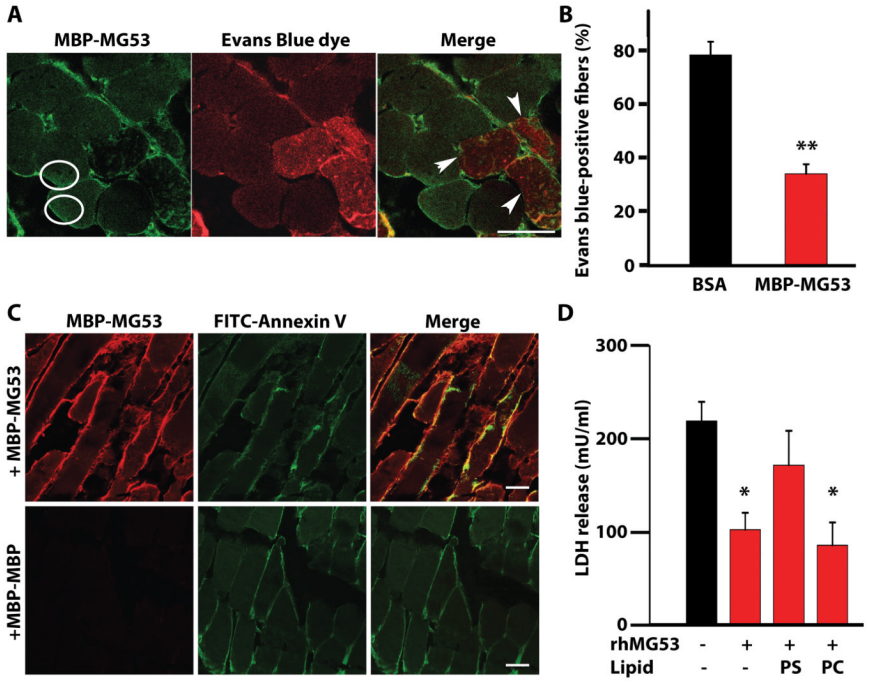

Figure 5. Cell membrane resealing mediated by rhMG53 requires binding to phosphatidylserine (PS)

(**A**) Mouse gastrocnemius muscles were co-injected with CTX, Evans blue dye, and either MBP-MG53 (20 μg/mL) or BSA. Sections were immunostained for MBP-MG53 and overlaid with images of Evans blue dye fluorescence. Circles surround areas of increased MBP-MG53 signal inside of muscle fibers. Arrows indicate fibers that lack MBP-MG53 decoration and contain Evans Blue dye. Scale bar, 20 μm. (**B**) Percentage of total muscle fibers displaying entry of Evans blue dye. Data are means ± SEM (n=24 sections) $^{**}P < 0.01$ by ANOVA. (**C**) Gastrocnemius muscles of wild-type mice were co-injected with CTX, MBP-MG53, and FITC-labeled Annexin V, which binds to PS. Cryosections were stained for MBP-MG53 and examined by confocal microcopy. Control mice were injected with MBP-MBP instead of MBP-MG53. Images are representative of 4-6 sections from three different experimental animals per group. Scale bars, 20 μm. (**D**) HEK293 cells were treated with rhMG53 and damaged by glass microbeads before measuring LDH release. Cells were simultaneously treated with PS or phosphatidylcholine (PC) to check competition with rhMG53 function. Data are means ± SEM (n=6-8 independent assays with the condition performed in triplicate in each experiment). $^{*}P < 0.05$ versus control without lipids or protein, ANOVA.

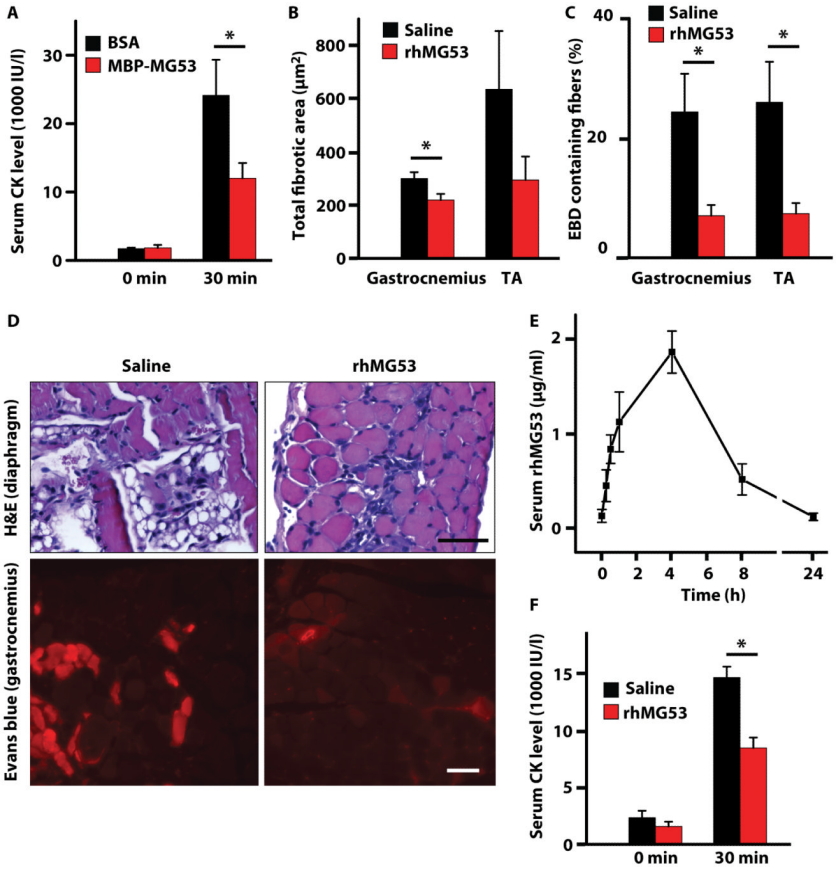

Figure 6. Recombinant MG53 protein therapy reduces pathology in the *mdx*dystrophic mouse model

(**A**) Resting CK levels (pre-running) were measured for 4-week–old *mdx* mice (n=4 per group) before they were injected intravenously with a single dose of either 4 mg/kg MBP-MG53 or with BSA as a control. These *mdx* mice were then exercised on a rodent treadmill with downhill running (15°) at 10 m/min for 90 min. CK levels were measured 30 minutes after completion of exercise. Data are means ± SEM. *P < 0.05 versus control by ANOVA. (**B**) Four-week–old *mdx* mice were injected twice daily for 4 days with either 8 mg/kg rhMG53 (n=6) or vehicle control (saline, n=8). Area of fibrosis was measured by ImageJ using hematoxylin & eosin–stained sections of gastrocnemius and tibialis anterior (TA) muscles. Data are means ± SEM, *P < 0.05 by t test. (**C**) Percentage of Evans blue dye–positive fibers measured using fluorescence microscopy of cryosections from gastrocnemius and TA of *mdx* mice treated with rhMG53 (n=4) or saline control (n=6). Data are means ± SEM, *P < 0.05 by t test. (**D**) Representative images of H&E-stained diaphragm muscles and fluorescence microscopy of Evans blue dye in gastrocnemius muscle from *mdx* mice following 4 days of indicated treatments. Scale bars, 50 μm. (E) MG53 in serum over time following subcutaneous (SC) injection of rhMG53 (2 mg/kg). Densitometry was quantified from Western blots from 3 animals. Data are means ± SEM. (F) Following SC injection of rhMG53 (8 mg/kg) or saline vehicle, *mdx* mice (n=6-8 per group) were subjected to downhill running (15°) at 10 m/min for 90 min. CK levels were measured from serum samples taken before running (0 m) at 30 min after the end of treadmill running (30 m). Data are means ± SEM, *P < 0.05 by t test.

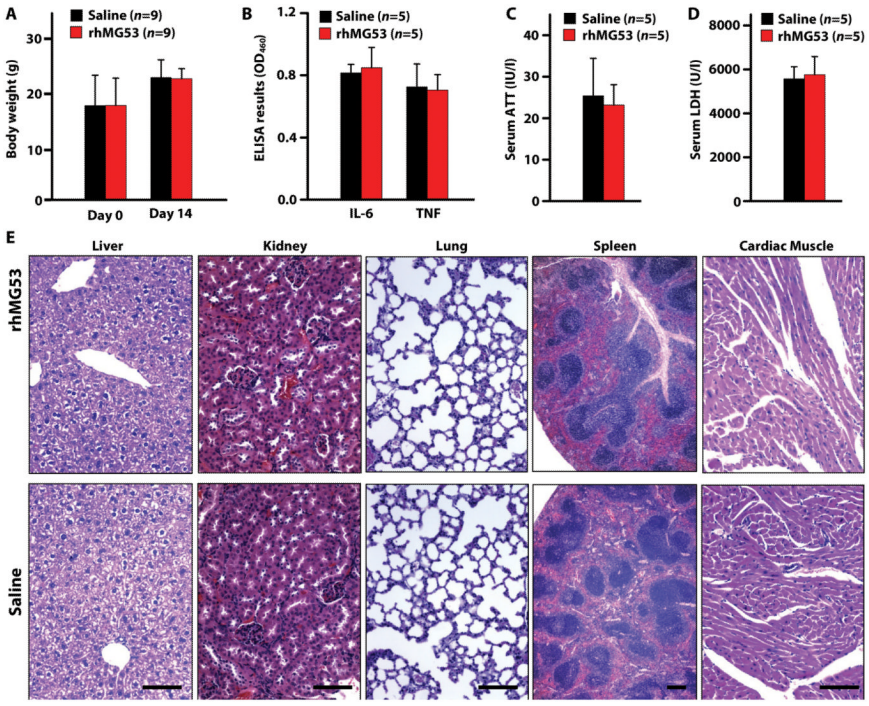

Figure 7. No detectable toxicity or inflammation occurs in *mdx* mice following SC injection of rhMG53

Cohorts of male *mdx* mice littermates were injected once daily for 2 weeks with 8 mg/kg rhMG53 or saline vehicle. After two weeks of injections the animals were sacrificed and serum and tissue samples were collected. (**A**) The body weight for animals injected with rhMG53. (**B**) Serum levels of inflammatory cytokines interleukin 6 (IL-6) and tumor necrosis factor α **(**TNFα) at day 14 after injection. Data are means ± SEM. (**C**) Levels of alanine aminotransferase (ATT) in the blood at day 14 after injection. Data are means ± SEM. (**D**) Measurement of LDH levels in the serum at day 14 after injection. Data are means ± SEM. (**E**) Representative H&E histology images of multiple tissue types from *mdx* mice injected with saline or rhMG53 (n = 5 per group) as described above. Scale bars, 100 μm.